tallized from methanol to give 142 mg (88%) of the unchanged starting material (**3**), mp 118–119 °C (mixture melting point).

B. Neat Thermolysis. A sample of **3** (0.64 g, 2 mmol) was heated at ca. 310 °C for 5 h and the resultant mixture was chromatographed over silica gel. Elution with petroleum ether gave 300 mg (45%) of the unchanged starting material (**3**), mp 118–119 °C (mixture melting point). Subsequent elution with a mixture (1:4) of benzene and petroleum ether gave 200 mg (36%) of **37**,[18] mp 101 °C, (mixture melting point), after recrystallization from methanol. Further elution of the column with benzene gave a small amount (20 mg, 9%) of benzoic acid, mp 121 °C (mixture melting point).

Thermolysis of 3-Benzyl-3,4,5-triphenyl-2(3*H*)-furanone (4) in Diphenyl Ether. A solution of **4** (0.8 g, 2 mmol) in diphenyl ether (10 mL) was refluxed for 1 h, and the solvent was removed under vacuum to give a residual solid, which was washed with petroleum ether and later recrystallized from a mixture (1:1) of benzene and petroleum ether to give 755 mg (95%) of the furanone **38**, mp 154–155 °C: IR ν_{max} (KBr) 3060, 3020, 2920 (CH), 1750 (C=O), 1600 (C=C) cm^{-1}; UV λ_{max} (methanol) 215 nm (ϵ 3560), 278 (1100).

Anal. Calcd for $C_{29}H_{22}O_2$: C, 86.56; H, 5.47. Found: C, 86.68; H, 4.99.

Thermolysis of 3,3′-Diphenyl[3,3′-bibenzo[*b*]furan]-2,2′(3*H*,3′*H*)dione (16). A sample of **16** (0.46 g, 1.1 mmol) in diphenyl ether (10 mL) was refluxed for 1 h. Removal of the solvent under vacuum gave a residual solid, which was chromatographed over silica gel. Elution of the column with a mixture (1:3) of benzene and petroleum ether gave 200 mg (42%) of the furanone **25**,[13,33] mp 113–114 °C (mixture melting point), after recrystallization from methanol.

In a repeat experiment, a sample of **16** (1.0 g, 2.3 mmol) was refluxed in cumene (10 mL) for 0.5 h. Removal of the solvent and recrystallization from methanol gave 680 mg (68%) of **25**, mp 113–114 °C (mixture melting point).

Thermolysis of 5,5′-Dimethyl-3,3′-diphenyl[3,3′-bibenzo[*b*]furan]-2,2′(3*H*,3′*H*)-dione (17) in Cumene. A sample of **17** (1.1 g, 2.3 mmol) in cumene (15 mL) was refluxed for 1 h. Removal of the solvent and recrystallization from methanol gave 675 mg (65%) of the furanone **26**, mp 105–106 °C (mixture melting point).

Thermolysis of 6,6′-Dimethyl-3,3′-diphenyl[3,3′-bibenzo[*b*]furan]-2,2′(3*H*,3′*H*)-dione (18) in Cumene. A sample of **18** (0.85 g, 2 mmol) in cumene (15 mL) was refluxed for 1 h and the solvent was removed under reduced pressure. The residue, thus obtained, was recrystallized from methanol to give 530 mg (62%) of **27**, mp 122 °C (mixture melting point).

Laser Flash Photolysis. The laser flash photolysis experiments were carried out in a computer-controlled setup using a Tachisto excimer (248 nm, Kr, F_2) and a Molectron UV-400 laser system. The system is fully interphased with a PDP 11/55 multiuser computer which controls the experiment, averages signals, and processes the data. The instrument allows the monitoring of transient phenomena in the 10 ns–100 μs time range. Details of the apparatus and the procedures are available in previous publications[33,34] from the Radiation Laboratory.

Pulse Radiolysis. For spectrophotometric pulse radiolsis, 5-ns electron pulses from the Notre Dame 7-MeV ARCO LP-7 linear accelerator were used at a dose rate of $\sim 2 \times 10^{16}$ (eV/g)/pulse. A description of the setup is available elsewhere.[35] The signals were recorded by a Biomation 6500 transient recorder interfaced with an LSI-11 microcomputer system.

Acknowledgment. We thank the Department of Science and Technology, Government of India, Indian Institute of Technology, Kanpur, and the Office of Basic Energy Sciences of the U.S. Department of Energy for financial support of this work. We are thankful to Dr. S. M. S. Chauchan for partial experimental assistance.

Registry No. 1, 18374-46-4; **2**, 2313-03-3; **3**, 31589-99-8; **4**, 92545-46-5; **5**, 6333-11-5; **6**, 849-01-4; **10**, 92545-47-6; **11**, 92545-48-7; **12**, 92545-49-8; **13**, 7404-46-8; **16**, 65425-10-7; **17**, 65425-11-8; **18**, 65425-12-9; **25**, 3117-37-1; **31**, 55190-56-2; **32**, 92545-53-4; **33**, 92545-52-3; **34**, 40237-73-8; **35**, 92545-50-1; **36**, 92545-51-2; benzophenone, 119-61-9.

(33) Das, P. K.; Encinas, M. V.; Small, R. D., Jr.; Scaiano, J. C. *J. Am. Chem. Soc.* **1979**, *101*, 6965–6970 and references therein.

(34) Das, P. K.; Bobrowski, K. *J. Chem. Soc., Faraday Trans. 2* **1981**, *77*, 1009–1027.

(35) (a) Patterson, L. K.; Lillie, J. *Int. J. Radiat. Phys. Chem.* **1974**, *6*, 129–141. (b) Schuler, R. H. *Radiat. Res.* **1977**, *69*, 417–433.

Colloidal Catalyst-Coated Semiconductors in Surfactant Vesicles: In Situ Generation of Rh-Coated CdS Particles in Dihexadecylphosphate Vesicles and Their Utilization for Photosensitized Charge Separation and Hydrogen Generation

Yves-M. Tricot and Janos H. Fendler*

Contribution from the Department of Chemistry and Institute of Colloid and Surface Science, Clarkson University, Potsdam, New York 13676. *Received May 14, 1984*

Abstract: Colloidal ca. 40-Å diameter CdS semiconductor particles were in situ generated and in situ coated by rhodium in 800–1000-Å diameter single-bilayer dihexadecylphosphate (DHP) vesicles. The vesicles controlled the size and the stability of the CdS particles, generated by H_2S from adsorbed Cd^{2+} ions. CdS fluorescence could be observed only from particles formed at the inside surface of the vesicles and when the sonication pH was higher than 6. No fluorescence could be detected in CdS colloids generated from Cd^{2+} added to already formed vesicles. Quenching of CdS fluorescence by methylviologen (MV^{2+}), Rh^{3+}, and thiophenol (PhSH), externally added or cosonicated with DHP, was determined. Externally added MV^{2+} and Rh^{3+} did not quench CdS fluorescence, but externally added PhSH did. Photolysis by visible light, in the absence of oxygen, of DHP-vesicle-stabilized, rhodium-coated colloidal CdS in the presence of PhSH as electron donor led to hydrogen formation which could be sustained until complete consumption of PhSH. Effects of temperature and PhSH and catalyst concentrations on the hydrogen production were determined. Turnover numbers, limited by the maximum tolerable amount of PhSH in the vesicles, were 5.4 and 13.6 for CdS and Rh, respectively.

The current approach to artificial photosynthesis[1–4] involves the separate optimizations of the sacrificial reduction and oxidation half-cells. In the reduction half-cell, hydrogen is generated at the expense of a sacrificial electron donor, D. In homogeneous solution, excitation of the sensitizer, S, is followed by electron transfer

(1) Grätzel, M. *Acc. Chem. Res.* **1981**, *14*, 376–384.
(2) Porter, G. *Proc. R. Soc. London, Ser. A* **1978**, *362*, 281–303.
(3) Calvin, M. *Acc. Chem. Res.* **1978**, *11*, 369–374.
(4) Fendler, J. H. *J. Phys. Chem.* **1980**, *84*, 1485–1491.

0002-7863/84/1506-7359$01.50/0

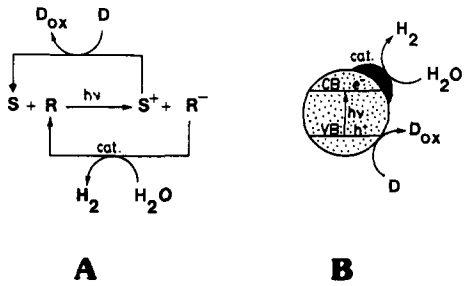

Figure 1. Basic features of sacrificial water reduction systems. (A) Homogeneous solution with sensitizer, S, electron relay, R, sacrificial electron donor, D, and catalyst. (B) Catalyst-coated colloidal semiconductor obviating the need for electron relay. Following band-gap excitation, conduction band (CB) electrons reduce water at the catalyst-coated semiconductor–water interface, while the electron transfer from D replenishes the positive holes in the valence band (VB).

to a relay, R. In the presence of a catalyst the reduced relay, R^-, is reoxidized to R, and the water is reduced to H_2. The function of the electron donor is to reform S from S^+ (Figure 1). Although this approach continues to be used and improved upon, replacement of the sensitizer and relay by dispersed colloidal semiconductors has gained widespread popularity.[1,5-42] Colloidal semiconductors offer a number of advantages. They are relatively inexpensive. They have broad absorption spectra and high extinction coefficients at appropriate band gap energies or, if needed, can be modified by derivatization or sensitizer adsorption. Importantly, electrons produced by band gap excitation can be used directly without relays for catalytic water reduction (Figure 1). Unfortunately, colloidal semiconductors also suffer from a number of disadvantages. They are notoriously difficult to form reproducibly as small (<200 Å in diameter) monodispersed particles. They are equally difficult to maintain in solution for extended times in the absence of stabilizers, which bound to affect their photoelectrical behavior unpredictably. Their modification and their loading by catalysts are, at present, more of an art than science. Furthermore, the lifetime of electron–hole pairs in semiconductors is orders of magnitude shorter than the excited-state lifetime of typical organic sensitizers. This is due to a very fast undesirable electron–hole recombination. Quantum yields for charge separations in colloidal semiconductors are, therefore, disappointingly low.

Incorporation of colloidal semiconductors into polyurethane films[43] and Nafion membranes[44] were reported to have overcome some of these disadvantages. Research in our laboratories is focussed upon the utilization of membrane mimetic systems[45,46] for realizing the full potential of colloidal semiconductors. Preliminarily, we have reported efficient photosensitized charge separation and hydrogen generation from in situ generated and in situ catalyst-coated colloidal semiconductors in reversed micelles[47] and surfactant vesicles.[48] These organized surfactant assemblies have provided compartments for the reproducible formation of long-lived, small, and uniform colloidal semiconductors and decreased the extent of unwanted electron–hole recombinations by creating high local concentration of appropriate quenchers. Details are provided in the present report on the optimization and characterization of rhodium-coated cadmium sulfide, in situ formed and stabilized in dihexadecylphosphate vesicles, for photosensitized hydrogen generation.

Experimental Section

Dihexadecylphosphate (DHP, Sigma), $CdCl_2 \cdot 2H_2O$ (Baker), $RhCl_3 \cdot 3H_2O$ (Alfa), methylviologen dichloride ($MVCl_2$, Aldrich), and NaOH (Fischer) were of analytical grade and used without further purification. Hydrogen sulfide (Matheson), 99.5% pure, and thiophenol (PhSH, Aldrich), 97% pure, were used as received. DHP vesicles were prepared, as described previously,[49] by sonication in water at 80 °C. Typically, 49.2 mg of DHP was sonicated in 25 mL of triply distilled water. After initial dispersion, appropriate amounts of 0.1 M NaOH, 0.1 M $CdCl_2$, and 0.1 M $RhCl_3$ were added using microsyringes. After

(5) Sakata, T.; Kawai, T. In "Energy Resources through Photochemistry and Catalysis"; Academic Press: New York, 1983; pp 322–358.
(6) Schrauzer, G. N.; Guth, T. D. *J. Am. Chem. Soc.* **1977**, *99*, 7189–7193.
(7) Krautler, B.; Bard, A. J. *J. Am. Chem. Soc.* **1978**, *100*, 4317–4318.
(8) Van Damme, H.; Hall, W. K. *J. Am. Chem. Soc.* **1979**, *101*, 4373–4374.
(9) Kiwi, J.; Borgarello, E.; Pelizetti, E.; Visca, M.; Gratzel, M. *Angew. Chem., Int. Ed. Engl.* **1980**, *19*, 646–648.
(10) Kawai, T.; Sakata, T. *Chem. Phys. Lett.* **1980**, *72*, 87–89.
(11) Pichat, J.; Mozzanega, M. N.; Disdler, J.; Herrmann, J.-M. *Nouv. J. Chim.* **1982**, *6*, 559–564.
(12) Lehn, J.-M.; Sauvage, J.-P.; Ziessel, R. *Nouv. J. Chim.* **1980**, *4*, 623–627.
(13) Sato, S.; White, J. M. *Chem. Phys. Lett.* **1980**, *70*, 83–86.
(14) Sato, S.; White, J. M. *J. Am. Chem. Soc.* **1980**, *102*, 7206–7210.
(15) Darwent, J. R.; Porter, G. *J. Chem. Soc. Chem. Commun.* **1981**, 145–146.
(16) Darwent, J. R. *J. Chem. Soc., Faraday Trans. 2* **1981**, *77*, 1703–1709.
(17) Harbour, J. R.; Wolkow, R.; Hair, M. L. *J. Phys. Chem.* **1981**, *85*, 4026–4029.
(18) Izumi, I.; Fan, F. F.; Bard, A. J. *J. Phys. Chem.* **1981**, *85*, 218–223.
(19) Sakata, T.; Kawai, T. *Nouv. J. Chim.* **1981**, *516*, 279–281.
(20) Dounghong, D.; Ramsden, J.; Gratzel, M. *J. Am. Chem. Soc.* **1982**, *104*, 2977–2985.
(21) Lehn, J. M; Sauvage, J. P.; Ziessel, R.; Hilaire, L. *Isr. J. Chem.* **1982**, *22*, 168–172.
(22) Mills, A.; Porter, G. *J. Chem. Soc., Faraday Trans. 1* **1982**, *78*, 3659–3669.
(23) Borgarello, E.; Kalynasundaran, K.; Gratzel, M. *Helv. Chim. Acta.* **1982**, *65*, 243–248.
(24) Sakata, T.; Kawai, T.; Hashimoto, K. *Chem. Phys. Lett.* **1982**, *88*, 50–54.
(25) Moser, J.; Grätzel, M. *J. Am. Chem. Soc.* **1983**, *105*, 6547–6555.
(26) Blondel, G.; Harriman, A.; Porter, G.; Kiwi, J. *J. Phys. Chem.* **1983**, *87*, 2629–2636.
(27) Matsumura, M.; Saho, Y.; Tsubomura, H. *J. Phys. Chem.* **1983**, *87*, 3807–3808.
(28) Curran, J. S.; Lamouche, D. *J. Phys. Chem.* **1983**, *87*, 5405–5411.
(29) Houlding, V. H.; Grätzel, M. *J. Am. Chem. Soc.* **1983**, *105*, 5695–5696.
(30) Duonghong, D.; Erbs, W.; Shuben, L.; Grätzel, M. *Chem. Phys. Lett.* **1983**, *95*, 266–268.
(31) Hashimoto, K.; Kawai, T.; Sakata, T. *Nouv. J. Chim.* **1983**, *7*, 249–253.
(32) Hope, G.; Bard, A. J. *J. Phys. Chem.* **1983**, *87*, 1979–1984.
(33) Disdier, J.; Herrmann, J. M.; Pichat, P. *J. Chem. Soc., Faraday Trans. 1* **1983**, *79*, 651–660.
(34) Grätzel, M.; Moser, J. *Proc. Natl. Acad. Sci. U.S.A.* **1983**, *80*, 3129–3132.
(35) Herrmann, J.-M.; Mozzanega, M.-N.; Pichat, P. *J. Photochem.* **1983**, 333–343.
(36) Yesodharan, E.; Grätzel, M. *Helv. Chim. Acta* **1983**, *66*, 2145–2153.
(37) Hashimoto, K.; Kawai, T.; Sakata, T. *Chem. Lett. Jpn.* **1983**, 709–712.
(38) Nishimoto, S.; Ohtami, B.; Kajiwara, H.; Kagiya, T. *J. Chem. Soc., Faraday Trans. 1* **1983**, *79*, 2685–2694.
(39) Ward, M. D.; White, J. R.; Bard, A. J. *J. Am. Chem. Soc.* **1983**, *105*, 27–31.
(40) Matthews, R. *Aust. J. Chem.* **1983**, *36*, 191–197.
(41) Magliozzo, R. S.; Krasna, A. I. *Photochem. Photobiol.* **1983**, *38*, 15–21.
(42) Serpone, N.; Borgarello, E.; Gratzel, M. *J. Chem. Soc. Chem. Commun.* **1984**, 342–344.
(43) Meissner, D.; Memming, R.; Kastening, B. *Chem. Phys. Lett.* **1983**, *96*, 34–37.
(44) Krishnan, M.; White, J. R.; Fox, M. A.; Bard, A. J. *J. Am. Chem. Soc.* **1983**, *105*, 7002–7003.
(45) Fendler, J. H. "Membrane Mimetic Chemistry"; Wiley-Interscience: New York, 1982.
(46) Fendler, J. H. *Chem. Eng. News* **1984**, *62*, 25–38.
(47) Meyer, M.; Wallberg, C.; Kurihara, K.; Fendler, J. H. *J. Chem. Soc., Chem. Commun. 1984*, 90–91.
(48) Tricot, Y.-M.; Fendler, J. H. *J. Am. Chem. Soc.* **1984**, *106*, 2475–2476.
(49) Tricot, Y.-M.; Furlong, D. N.; Sasse, W. H. F.; Snook, I.; Van Megan, W. *J. Colloid Interface Sci.* **1984**, *97*, 380–391.

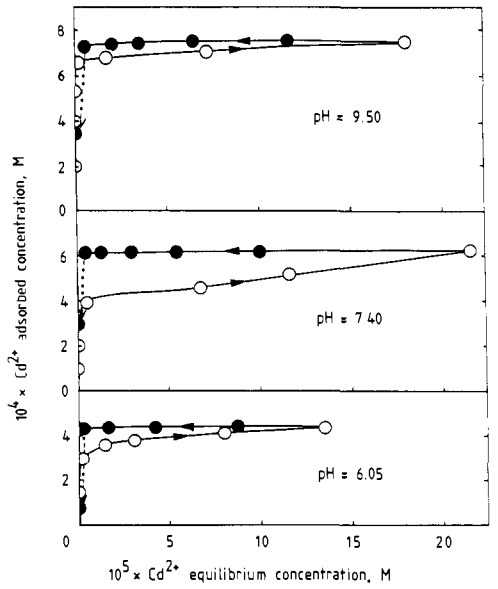

Figure 2. Adsorption and desorption isotherms at room temperature of Cd^{2+} in 2×10^{-3} M DHP vesicles sonicated at three different pHs. (-O→O-) Adsorption isotherm, (-●←●-) desorption (dialysis by ultrafiltration), (- - →) passage through cation exchange resin.

sonication for approximately 30 min with an output power of 50–60 W (or until the turbidity had reached a constant value), traces of titanium released by the microtip were removed by centrifugation (table-top model, 3000 rpm). The volume of the vesicle dispersions was adjusted usually to 45 mL, to give a final DHP concentration of 2×10^{-3} M, at which the pH was determined (pH referred subsequently to as "sonication pH"). When desired, externally adsorbed or nonadsorbed cations were removed by passing the dispersions through a Bio-Rad AG-50W-X2 (100–200 mesh, hydrogen form) cation exchange resin column. The resin was always replaced before 5% of its capacity was used. In order to concentrate the dispersions or to remove HCl resulting from the acid cation exchange resin treatment, an Amicon ultrafiltration stirred cell of 65-mL maximum capacity, equipped with a Diaflo membrane of 100 000 nominal molecular weight cutoff (type XM-100A), was used. The same technique was used to determine the absorption isotherms of Cd^{2+} on the DHP vesicles, as described elsewhere.[50] The concentrations of Cd^{2+} ions in the filtrates (equilibrium concentrations of the adsorption isotherms) were measured by atomic absorption spectroscopy, using a Perkin-Elmer 290B atomic absorption instrument. The entrapped amounts of Cd^{2+} inside of the vesicles (or more precisely the nonremovable fractions of Cd^{2+} by cation exchange resin treatment) were also determined by atomic absorption and correlated with the absorbance of subsequently formed CdS, measured on a Hewlett-Packard 8450A diode array spectrophotometer. Colloidal CdS was formed by gently introducing excess H_2S above the surface of degassed DHP vesicle dispersions having Cd^{2+} adsorbed at the water–DHP interfaces. Fluorescence spectra of CdS were recorded on a Spex Fluorolog spectrofluorimeter and were not corrected for the response of the photomultiplier tube. Hydrodynamic radii of vesicles were determined by dynamic light scattering at 90°, using an Ar ion laser, goniometer, and autocorrelator system previously described.[51] Flash photolysis experiments were carried out using the third harmonic (λ = 355 nm) of a Nd:YAG laser (Quanta Ray DCR-1A) for excitation and a 150-W xenon lamp for the analyzing light, as previously described.[51] Electron micrographs were obtained on a Phillips EM 200 instrument. Vesicle solutions were, without any staining, evaporated on a 200 mesh copper grid (Formvar support).

Vesicle dispersions, 25 mL, were photolyzed under anaerobic conditions by a 450-W xenon lamp using 350-nm cutoff and water filters. Rhodium coating of the colloidal CdS was achieved either by UV irradiation for 1 h of coadsorbed Rh^{3+} before injection of the electron donor PhSH or in the presence of PhSH under visible light irradiation. Reduction of Rh^{3+} to Rh^0 was followed by absorbance (scattering) changes between 350 and 700 nm.[48] Hydrogen generation was determined in the gas phase by gas chromatography, using a Hewlett-Packard 7620A chromatograph. Gas samples were analyzed through a Molecular sieve 5A 100/120 mesh metal column (5 ft × $^1/_8$ in.), maintained at 60 °C. Argon was used as carrier gas, under 30 psi of initial pressure and at a flow rate of 30 mL/min. The retention times were approximately 2 min for H_2, 4 min for O_2, and 7 min for N_2. Gases were detected via a thermal conductivity bridge (Model HP 7655A, set at 150 mA). Calibration of the instrument was done with a standard gas mixture of 2% H_2 in Ar (Matheson). Sample volumes were in the range 10–100 μL.

(50) Tricot, Y.-M.; Furlong, D. N.; Sasse, W. H. F. *Aust. J. Chem.* **1984**, *37*, 1147–1156.
(51) Reed, W.; Guterman, L.; Tundo, P.; Fendler, J. H. *J. Am. Chem. Soc.* **1984**, *106*, 1897–1907.

Table I. Effects of Sonication pH on CdS Formation in DHP Vesicles[a]

	nonremovable fraction of Cd^{2+},[c] %		relative fluorescence intensity of CdS at 500 nm,[e] arbitrary units	
pH at sonication[b]	atomic absorption[c]	CdS absorbances[d]	Cd^{2+} on both sides	Cd^{2+} left after cation exchange
3.22	100	100	5	5
3.82	100	100	5	5
4.80	69	63	11	22
6.07	58	47	88	64
6.86	56	53	100	80
8.93	43	39	100	32

[a] [DHP] = 2×10^{-3} M, [Cd^{2+}] = 2×10^{-4} M, stoichiometric. [b] Bulk pH, determined by a combination electrode using a Radiometer PHM 26 pH meter. [c] Taking the ratio of Cd^{2+} prior and subsequent to passages through a cation exchange resin. [d] Converting the Cd^{2+} to CdS (by exposure to H_2S) prior and subsequent to passages through a cation exchange resin and measuring the 400-nm absorbance (due to CdS). [e] λ_{ex} = 330 nm.

Results

Optimization of Preparation Conditions. The role of vesicles is to control the size of in situ generated CdS colloidal particles and to stabilize them. For this purpose, one has to make sure that no significant amount of the CdS precursor, Cd^{2+}, is dispersed in the bulk solution. Moreover, the permeability of the DHP membranes has to be known in order to control the location of Cd^{2+}, either on the inside or on the outside surfaces of the vesicles. Figure 2 shows adsorption isotherms of Cd^{2+}, externally added to DHP vesicles formed by sonication at different pH values. The ultrafiltration technique used allows us to measure both the adsorption and the desorption of the cations, the latter being done by progressively replacing the equilibrium solution with distilled water. At the end of the process, when the equilibrium concentration was found to be very small, penetration of Cd^{2+} ions into vesicles was tested by means of the cation-exchange resin treatment. The results revealed the essentially complete adsorption of up to 3×10^{-4} M Cd^{2+} at all three pH investigated,[51] presumably on the outside surface of the vesicles. Differences in the three isotherms can be rationalized in terms of increased permeabilities of the DHP membrane toward cations with increasing pH values of the solution during sonication. At pH 6.05, very little Cd^{2+} diffused through the vesicles, as reflected by a single adsorption plateau and by the fact that almost all of Cd^{2+} was removed by the cation exchange resin. At pH 7.40, penetration occurred but only at Cd^{2+} equilibrium concentrations higher than 5×10^{-5} M and a second adsorption plateau was reached. After desorption (which actually did not show any desorption but only reduction of the equilibrium concentrations) the cation exchange resin treatment revealed that about 50% of the Cd^{2+} had diffused inside of the vesicles, but did not leak during the residence time in the resin column. At pH 9.50, the second adsorption plateau, corresponding to adsorption on both interfaces, was directly reached. However, internally adsorbed Cd^{2+} (or more exactly $Cd(OH)^+$ at this high pH) was still not removed by the cation exchange resin treatment. These results showed that with 2×10^{-4} M Cd^{2+} (and 2×10^{-3} M DHP), no appreciable Cd^{2+} remained in the bulk and that the CdS resides only at the DHP–water interface. Furthermore, at pH 7, diffusion of Cd^{2+} across the DHP membrane did not occur, unless the equilibrium concentration was high, and it was, therefore, possible to localize specifically Cd^{2+} on either side of the vesicles.

The sonication pH had further effects on the interaction of Cd^{2+} with the vesicles and on the properties of subsequently formed CdS (Table I). The onset of colloidal CdS absorbance, 520 nm,

Table II. Effects of the Initial Cd^{2+} Concentration on CdS Formation[a]

initial $10^4[Cd^{2+}]$, M	Cd^{2+}:DHP ratio	nonremovable fraction of Cd^{2+},[b] %	relative fluorescence intensity of CdS at 500 nm,[c] arbitrary units: Cd^{2+} on both sides	relative fluorescence intensity of CdS at 500 nm,[c] arbitrary units: Cd^{2+} left after cation exchange
0.5	1:40	46	45	22
1.0	1:20	43	80	50
2.0	1:10	50	100	75
3.0	1:6.7	58	94	81
4.0	1:5	66	83	88
5.0	1:4	75	87	76

[a] At constant [DHP] = 2×10^{-3} M, pH 7.0. [b] Determined by atomic absorption spectroscopy and by CdS absorption. [c] λ_{ex} = 330 nm.

corresponded to band gap excitation of 2.4 eV as reported for CdS in various systems.[16,20,52] The optical density rose steeply toward the ultraviolet, with no peak, and 400 nm was arbitrarily chosen to measure an extinction coefficient, as was done by other workers.[20,52] The extinction coefficient of CdS formed with different sonication pH was determined to be $\epsilon_{400\,nm} = 900 \pm 100$ M^{-1} cm^{-1}, from the Cd^{2+} concentration measured by atomic absorption and from the absorbance of the CdS formed by assuming complete reaction with H_2S. This value showed no significant dependence on the sonication pH and on the location of CdS (inside or on both sides of the vesicles). When cosonicated with DHP, Cd^{2+} appeared to be more strongly adsorbed to the DHP membrane at low (3–4) than at high pH (above 7). This manifested in the inability of the cation exchange resin to remove Cd^{2+} at low pH, whereas, under the same conditions, 50–60% of Cd^{2+} could be removed at pH 7 or higher. This pH-dependent interaction of Cd^{2+} with the DHP membrane also correlated with the fluorescence of CdS, formed by H_2S exposure of the vesicle-adsorbed Cd^{2+}. The intensity of CdS fluorescence at 500 nm, from using 330-nm excitation, was maximized for a sonication pH of 7 or higher. This was not, however, a direct pH effect, since changes of pH after sonication of the surfactant did not influence CdS fluorescence. Interestingly, CdS formed exclusively at the outer surface of DHP vesicles did not show any fluorescence regardless of the pH (adjusted either during sonication or subsequent to it). The presence of Cd^{2+} during vesicle formation seemed, therefore, necessary to produce fluorescing colloidal CdS particles. The decrease of the relative intensity of CdS fluorescence, observed at high pH in vesicles that had CdS only at their interiors (last column in Table I), was merely due to the decrease of CdS concentration resulting from the cation exchange resin treatment.

Table II summarizes the effects of varying the ratio of Cd^{2+} to DHP on the entrapment of Cd^{2+} and on CdS fluorescence. Earlier work[49] showed that for MV^{2+} in DHP vesicles, increasing the amount of MV^{2+} resulted, as expected, in increased MV^{2+} entrapment up to a saturation point. Table II shows that it was the reverse for Cd^{2+}; i.e., when more Cd^{2+} was initially present at sonication, less Cd^{2+} could be removed by the cation exchange resin. This suggested that the binding of Cd^{2+} to the DHP–water interface became more pronounced as the Cd^{2+} concentration increased. The fluorescence intensity of CdS showed a linear increase only up to a Cd^{2+}/DHP ratio of 1:10 then stabilized or even decreased slightly, regardless whether CdS was located on both sides or only inside of the vesicles. This saturation effect probably arose from a self-quenching interaction of the colloidal CdS particles. Variation of the concentration of vesicles at constant Cd^{2+}/DHP ratio of 1:10 showed that the fluorescence intensity of CdS increased up to a CdS concentration of 5×10^{-4} M and decreased at higher concentration. This might be a trivial effect due to the scattering of the vesicles, as the turbidity increased at higher concentrations and also due to the high CdS absorbance.

(52) Ramsden, J. J.; Grätzel, M. *J. Chem. Soc., Faraday Trans. 1* **1984**, *80*, 919–933.

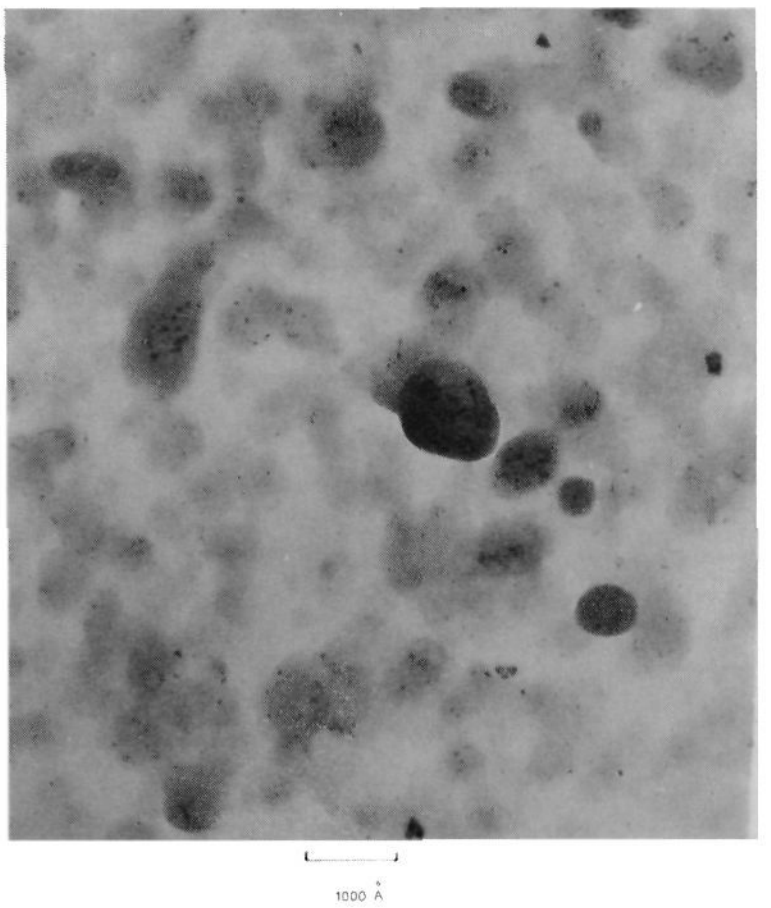

Figure 3. Electron micrograph of DHP-vesicle-stabilized, in situ generated, colloidal CdS.

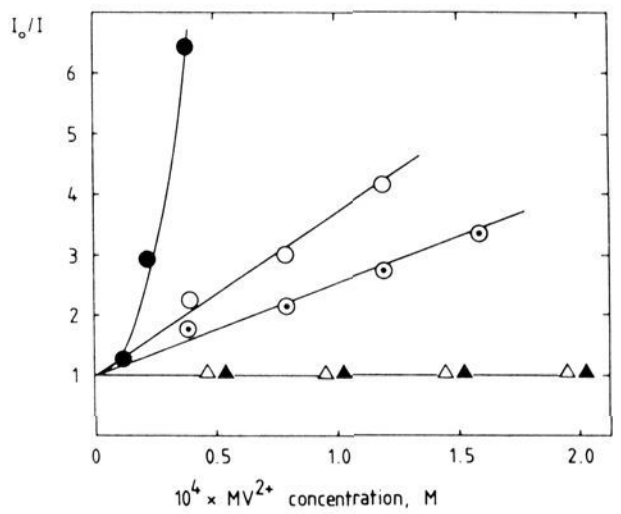

Figure 4. Quenching of CdS (2×10^{-4} M) fluorescence in DHP (2×10^{-3} M) vesicles by MV^{2+} in different locations: (●) CdS and MV^{2+} only inside; (○) CdS and MV^{2+} are on both sides, 30 min after CdS formation; (⊙) same samples, 8 days after CdS formation; (△) CdS inside only, MV^{2+} outside only; (▲) CdS on both sides, MV^{2+} outside only. λ_{ex} = 330 nm, λ_{em} = 500 nm.

In a preliminary communication,[48] we estimated that a few thousand Cd atoms were adsorbed on the surface of each vesicle and assumed that, after reaction with H_2S, the CdS would eventually aggregate to a single particle. This assumption turned out to be wrong, as shown by the electron micrographs in Figure 3. There were many colloidal CdS particles per vesicles, and their diameter was ca. 40 Å. It was not possible, though, to determine from the electron micrographs if the particles were only attached to the DHP–water interfaces or were embedded in the membrane. The vesicles themselves showed a size distribution in the 200–600-Å radii range. Dynamic light scattering measurements of DHP vesicles prepared from 2.0×10^{-3} M surfactant in the absence and in the presence of up to 7×10^{-4} M CdS particles gave hydrodynamic radii in the 500–600-Å range. These values corresponded well to those seen in Figure 3.

Fluorescence Quenching Experiments. Under band gap excitation (330 nm in our experiments), in situ generated colloidal CdS in DHP vesicles exhibited a weak fluorescence with a maximum near 500 nm, as reported previously.[48] The true fluorescence maximum could have been at slightly longer wavelength, since the spectra were not corrected. No significant difference was observed when $Cd(NO_3)_2$ replaced $CdCl_2$.

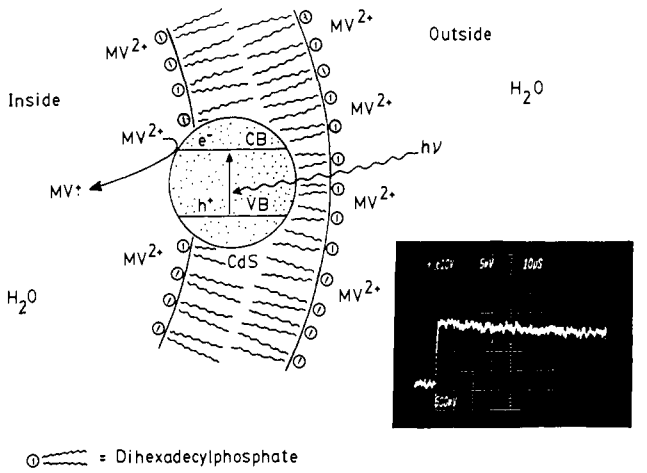

Figure 5. An idealized mechanism of photoinduced electron transfer from CdS conduction band to methylviologen (MV^{2+}), resulting in formation of methylviologen radical cation ($MV^{+\cdot}$). The colloidal CdS particle, as represented, was generated at the inside surface of the DHP vesicle. Its exact location is based on fluorescence quenching experiments (Figures 4, 6, and 7). Insert: oscilloscope trace showing the formation of $MV^{+\cdot}$ by the absorbance change at 396 nm, after a laser pulse at 355 nm.

Therefore, $CdCl_2$ was used for all subsequent experiments. Fluorescence of in situ generated colloidal CdS was found to be quenched by electron acceptors (MV^{2+} and Rh^{3+}) and by an electron donor (PhSH) arranged in a number of different combinations.

Figure 4 summarizes the quenching of CdS fluorescence in DHP vesicles by MV^{2+}. The highest quenching efficiency was obtained when both CdS and MV^{2+} were located only inside of the vesicles. Deviation from the Stern–Volmer relation (Figure 4) indicated the possibility of static quenching. Conversely, Stern–Volmer behavior was observed when CdS and MV^{2+} were distributed symmetrically on both sides of the vesicles (Figure 4). However, this quenching was time dependent. The apparent Stern–Volmer constant, determined 30 min after the in situ CdS formation, was $2.72 \times 10^4\ M^{-1}$ but decreased to $1.52 \times 10^4\ M^{-1}$ after 8 days of incubation at room temperature. When MV^{2+} was added after the in situ CdS formation in the DHP vesicles, no quenching was observed, regardless of the location of CdS colloidal particles. Direct evidence of this electron-transfer quenching was substantiated by laser flash photolysis (Figure 5). Excitation of CdS at 355 nm led to the formation of reduced methyl viologen ($MV^{+\cdot}$), as observed by the absorbance change at 396 and 605 nm. No fast back reaction of $MV^{+\cdot}$ with the CdS hole occurred, indicating that $MV^{+\cdot}$ did not remain at the CdS surface.

Figure 6 shows the quenching of CdS fluorescence by Rh^{3+}. We reported recently[48] this quenching when both CdS and Rh^{3+} were located only inside of the vesicles. However, the exact concentration of entrapped Rh^{3+} was not known, thus making questionable an estimation of the Stern–Volmer constant. Figure 5 shows the quenching effects of Rh^{3+} in known concentrations, when Rh^{3+} is located on both sides or just on the outside of the vesicles. Like in the case of MV^{2+}, quenching was observed only when Rh^{3+} was present during sonication, (i.e. only vesicle-entrapped Rh^{3+} quenched the CdS fluorescence). The plot of fluorescence intensity vs. Rh^{3+} concentration deviated from linearity. Nevertheless, taking the initial part of the quenching plot gave an apparent Stern–Volmer constant of $6.93 \times 10^4\ M^{-1}$. This quenching was not time dependent.

Different results were observed on using PhSH as quencher (Figure 7). Externally added PhSH was found to quench efficiently the DHP-vesicle-contained CdS. The quenching plot deviated from Stern–Volmer behavior, particularly when CdS was distributed on both sides of the vesicles. No time-dependent fluorescence change was found 30 min after PhSH addition except that the vesicles were slowly destabilized with addition of 1.5×10^{-3} M or more PhSH (at 2×10^{-3} M DHP concentration).

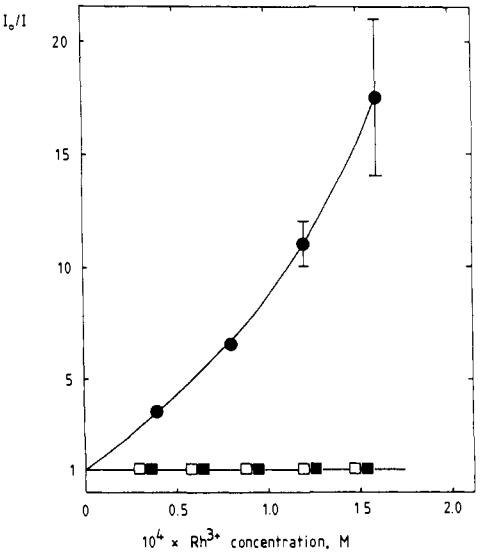

Figure 6. Quenching of CdS (2×10^{-4} M) fluorescence in DHP (2×10^{-3} M) vesicles by Rh^{3+} in different locations: (●) CdS and Rh^{3+} on both sides (both 30 min and 7 days after CdS formation); (□) CdS only inside, Rh^{3+} only outside; (■) CdS on both sides, Rh^{3+} only outside. λ_{ex} = 330 nm, λ_{em} = 500 nm.

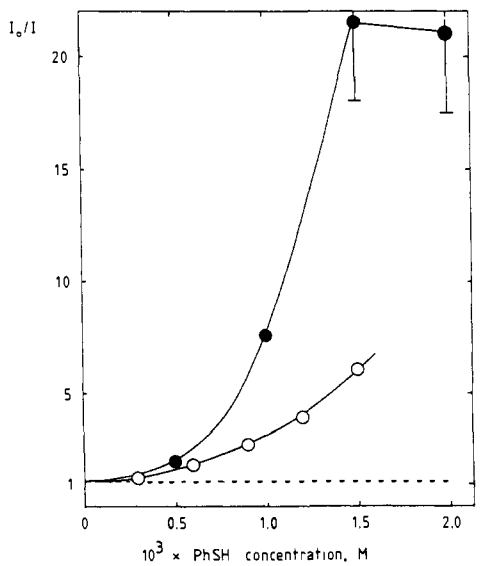

Figure 7. Quenching of CdS (2×10^{-4} M) fluorescence in DHP (2×10^{-3} M) vesicles by externally added PhSH in different locations: (●) CdS on both sides; (○) CdS inside only; (---) same quenching for CdS in AOT microemulsion.[47] λ_{ex} = 300 nm, λ_{em} = 500 nm.

Quenching of vesicle-incorporated CdS fluroescence is rationalized by the diffusion of the hydrophobic PhSH inside of the vesicle bilayers.

Hydrogen Generation Experiments. In a recent communication,[48] we have shown that rhodium-coated, vesicle-entrapped colloidal CdS could generate hydrogen under visible light ($\lambda > 350$ nm) irradiation in the presence of PhSH as electron donor. The results described in the previous sections demonstrate that it is not necessary to locate the CdS particles selectively inside of the vesicles in order to get photochemically active and physically stable colloidal CdS dispersions. The same hydrogen production activity was found whether the colloidal CdS was located only in the inside or on both sides of the vesicles (that is, the absolute rate of hydrogen formation was about twice as big in vesicles from which the external Cd^{2+} had not been removed than in those that contained CdS only in their inside). When generated from externally added Cd^{2+} (and Rh^{3+}) to preformed vesicles, rhodium-coated colloidal CdS was also active for hydrogen production, even not showing any fluorescence. The photochemical activity ap-

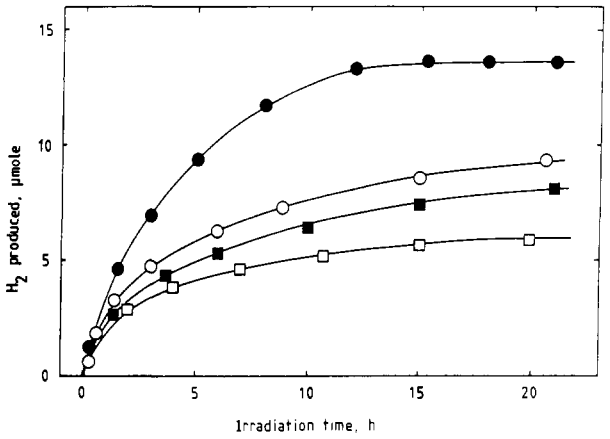

Figure 8. Hydrogen production in deaerated solutions as a function of irradiation time and temperature, using 350-nm cutoff and water filters. Plotted are the amounts of hydrogen produced in 25 mL of DHP vesicle solution and measured in the gas phase (16 mL) by GC: 2×10^{-3} M DHP, 2×10^{-4} M CdS symmetrically distributed on both sides of the vesicles, 8×10^{-5} M rhodium, reduced by UV irradiation prior to injection of 10^{-3} M PhSH as electron donor; pH approximately 7 at sonication and during photolysis. Temperatures: (●) 25 °C, (○) 30 °C, (■) 36 °C, (□) 44 °C.

peared to be independent of the fluorescence quantum yield. However, the reproducibility of hydrogen production was poor, probably due to an inhomogeneous mixing of the ions with the DHP vesicles. This was possible if the adsorption of Cd^{2+} and Rh^{3+} took place before the ions were homogeneously mixed in the bulk of the solution. The presence of these ions during sonication and formation of the vesicles ensured complete mixing of all the components, and the hydrogen production reproducibility was better than 10%. Aging of samples after CdS formation also resulted in decreased activity, presumably due to a slow photodecomposition of CdS, particularly in the presence of oxygen. All reported hydrogen production experiments were started within hours after CdS formation, and with the colloidal CdS located on both sides of the vesicles. The preparation of symmetrically organized colloidal CdS in DHP vesicles is also simpler since it obviates the need for cation exchange resin treatment and subsequent removal of HCl by ultrafiltration dialysis.

Hydrogen generation in vesicles that contain symmetrically organized CdS particles was examined as a function of temperature, catalyst concentration, electron-donor concentration, and mode of Rh^{3+} reduction. Figure 8 shows the effect of temperature on H_2 production as a function of irradiation time (with 350-nm cutoff filter). Rhodium coating of CdS was achieved by 1-h UV irradiation prior to injection of PhSH (2.60 μL of liquid PhSH, giving 10^{-3} M PhSH in a 25-mL photolysis sample). The highest rate was obtained at 25 °C, producing 13.6 μmol of hydrogen after 15 h of irradiation. Introducing additional PhSH resumed the hydrogen generation but at a strongly reduced rate. Further addition of the electron-donor destabilized the vesicles presumably by saturation of the bilayer with PhSH or by its oxidation product, PhSSPh. At the highest tolerable PhSH concentrations, turnover numbers of 5.4 and 13.6 were determined for CdS and Rh, respectively.

The effect of UV irradiation generated catalyst concentration is shown in Figure 9. At 25 °C, a maximum hydrogen generation rate was obtained on using 8×10^{-5} M Rh^{3+} (with 2×10^{-4} M CdS and 2×10^{-3} M DHP). Addition of more rhodium did not improve this rate, but less rhodium appeared less efficient. Blank experiments are also shown in Figure 9, either with CdS and no rhodium, 8×10^{-5} Rh^{3+} and no CdS, or neither rhodium nor CdS, but always in the presence of 10^{-3} M of PhSH. CdS alone produced small amounts of hydrogen. Almost none was detected during the other blank experiments. The necessity of visible light irradiation was also checked. If the irradiation was turned off during photolysis, hydrogen generation stopped after a few minutes (corresponding presumably to equilibration between liquid and

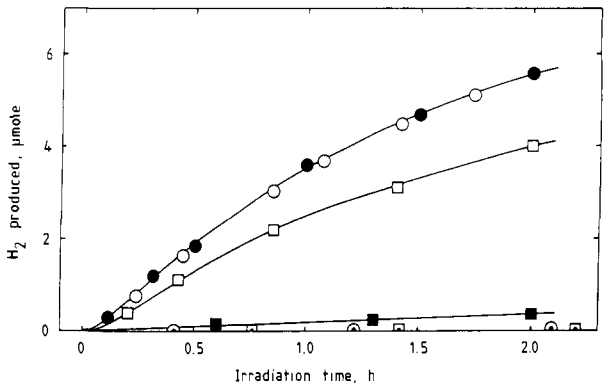

Figure 9. Hydrogen production at 25 °C in deaerated solutions as a function of catalyst (rhodium) concentration (UV reduced) during the first 2 h of irradiation using 350-nm cutoff and water filters, in the presence of 10^{-3} M of PhSH as electron donor. Other conditions as in Figure 7. (●) Rh 1.2×10^{-4} M, (○) Rh 0.8×10^{-4} M, (□) Rh 0.4×10^{-4} M, (■) no Rh, (□) no Rh and no CdS (only PhSH), (⊙) Rh^{3+} (unreduced) and no CdS (with PhSH).

Table III. H_2 Production in Rhodium-Coated, in Situ Generated, DHP-Vesicle-Stabilized, Colloidal CdS[a]

	max rate, μmol/h	irradn time at max rate, h	total amount of H_2 produced after 20 h, irradtn, μmol
Temperature Effect[b]			
temp, °C			
25	4.76 ± 0.20	0.20 ± 0.05	13.60
30	3.17 ± 0.20	0.40 ± 0.10	9.20
36	2.73 ± 0.30	0.40 ± 0.10	8.10
44	2.23 ± 0.20	0.50 ± 0.10	5.90
Effect of Rh^{3+} Concentration at 25 °C[b]			
$10^4[Rh^{3+}]$, M			
0.0	0.18 ± 0.01		0.35
0.4	3.31 ± 0.20	0.30 ± 0.10	
0.8	4.12 ± 0.20	0.40 ± 0.10	13.60
1.2	4.35 ± 0.20	0.40 ± 0.10	
Effect of PhSH Concentration at 25 °C[c]			
10^4[PhSH], M			
0.0	0.01		0.10
2.0	2.61 ± 0.20	0.45 ± 0.10	3.50
5.0	3.57 ± 0.20	0.60 ± 0.10	7.40
10.0	4.50 ± 0.20	0.60 ± 0.10	13.50

[a] Using 10^{-3} M PhSH unless otherwise stated. [b] UV reduction of 3.0×10^{-4} M stoichiometric Rh^{3+}. [c] No prior UV reduction of Rh^{3+}.

gas phases) and the amount of hydrogen measured in the gas phase remained constant for at least 2 h. Upon renewed irradiation hydrogen generation resumed at the previous rate.

Preparation of the samples could be simplified further by omitting the UV reduction of Rh^{3+} in DHP vesicles prior to the injection of PhSH. Hydrogen was generated at an almost identical rate by starting the visible light irradiation with samples containing Rh^{3+}, PhSH, and CdS in symmetrically organized DHP vesicles. The only difference was a short induction period (ca. 15 min) when Rh^{3+} was not reduced prior to PhSH injection (see also Table III, discussed below). About 13.5 μmol of hydrogen was generated, both in the absence and in the presence of prior UV irradiation of Rh^{3+}. Initial injection of 25 μmol of PhSH in the photolysis cell might be expected to yield a maximum of 12.5 μmol of hydrogen, assuming 100% conversion. Production of 13.5 μmol of hydrogen indicated the presence of some electron donor(s) in addition to PhSH. Figure 10 shows the effect of the initial PhSH concentration on the hydrogen production at 25 °C without UV irradiation of Rh^{3+} prior to injection of PhSH. These results are also summarized in Table III. The total amount of hydrogen generated decreased according to the decrease of PhSH initial concentration but was systematically about 1 μmol higher than the maximum expected amount. The initial rate decreased as it was expected from the CdS fluorescence quenching by PhSH

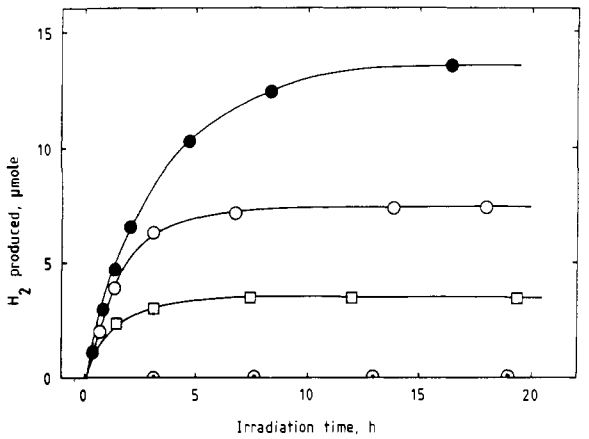

Figure 10. Hydrogen production at 25 °C in deaerated solutions as a function of PhSH (electron donor) concentration and irradiation time, using 350-nm cutoff and water filters. No UV reduction of 8×10^{-5} M Rh^{3+}; other conditions as in Figure 7. (●) PhSH 10^{-3} M, (○) PhSH 5×10^{-4} M, (□) PhSH 2×10^{-4} M, (⊙) no PhSH.

(Figure 7 and Table III). Without any PhSH, however, no hydrogen was detected, suggesting that PhSH was necessary to induce rhodium reduction.

The difference between UV-reduced and PhSH/visible light reduced catalyst toward hydrogen generation is also shown in Table III. At 25 °C and with 10^{-3} M PhSH, the maximum rate was attained after approximately 0.20 h when Rh^{3+} was UV reduced but only after approximately 0.60 h in the absence of UV reduction. However, the total amounts of produced hydrogen became equal after 2 h of visible light irradiation.

Discussion

Surfactant vesicles have been shown to be eminently useful media for generating and stabilizing colloidal semiconductors used in artificial photosynthesis. Advantage was taken of the unique ability of vesicles to compartmentalize colloidal CdS particles and their precursors. Negatively charged DHP vesicle surfaces ensured the efficient binding of Cd^{2+} in a controllable manner. Minimal CdS particle–particle interaction occurred, as indicated by the optimal fluorescence intensity, in systems that contained 10 surfactant head groups for each Cd^{2+}. Assuming statistical distribution, the average distance between the cations on the vesicle surface was approximately 60 Å. Exposure to H_2S resulted in nucleation at numerous sites. Collisions with neighboring CdS molecules, presumably at the vesicle surfaces, resulted in cluster formation. Conceivably, hydrophobic interactions stabilized the clusters and pulled then into the vesicle bilayers. Space and cadmium concentration restrictions were responsible, ultimately, for limiting the growth of CdS particles in the vesicle matrix. Electron micrography (Figure 3) indicates the average diameter of DHP vesicle associated CdS particles to be approximately 40 Å. Colloidal semiconductors in the 40–60-Å diameter range have been suggested to be ideal for photochemical solar energy conversion.[20] Assuming similar interatomic distances to those in crystalline cubic CdS, a 40-Å diameter CdS particle would contain approximately 1300 CdS molecules. One typical DHP vesicle of 1000-Å diameter contains about 80 000DHP surfactants, taking 70 $Å^2$ as surfactant heat-group area. With the usual ratio of one Cd^{2+} per ten DHP surfactants, a 1000-Å diameter vesicle would stabilize about six CdS particles. This value could vary considerably according to the size distribution of the DHP vesicles and the CdS particles but is in fair agreement with the electron micrograph (Figure 3).

In situ generation of CdS particles in DHP vesicles was easy and reproducible. Neither the amount nor the rate of H_2S addition to the Cd^{2+}-containing DHP vesicles was found to be too critical. Conversely, reproducible preparation of hexametaphosphate-stabilized colloidal CdS in water has met with considerable difficulties. DHP-incorporated colloidal particles were optically transparent and showed unprecedented stabilities. Their hydrodynamic diameters remained unaltered for months. This is a considerable improvement over the previously reported reversed micelle entrapped platinized CdS system.[47] Rapid exchange of the contents of the surfactant-entrapped water pools in apolar solvents[53-55] caused the growth of CdS particles in reversed micelles. The growth could only be controlled by having a large number of empty reversed micelles, which diminished, of course, the overall concentration of CdS, hence the efficiency of light harvesting.[47]

Absorption of visible light promotes an electron from the valence to the conduction band and thus creates an electron–hole pair in the semiconductor:

$$CdS \xrightarrow{h\nu} e^- + h^+ \qquad (1)$$

The charged cariers rapidly move about in the semiconductor frequently hitting the surface and each other. Electron–hole recombination, in the absence of quenching results in radiationless transition and in the emission of green light:[52,55,63]

$$e^- + h^+ \begin{cases} \nearrow \text{thermal recombination} \\ \searrow h\nu \end{cases} \qquad (2)$$

Fluorescence intensities of freshly prepared undoped CdS samples were extremely weak ($\Phi < 10^{-4}$).[60] It is important to reemphasize the lack of observable fluorescence of CdS particles located at the exterior of DHP vesicles. Apparently, the different environments at the inner and outer vesicle interfaces manifested in different behavior of CdS particles. Conceivably, those residing at the outer surface were protected to a lesser extent than those entrapped in the vesicles. In accord with this hypothesis was the lack of observable fluorescence of CdS particles in water in the absence of added stabilizers. Furthermore, no increase in fluorescence intensity or change in emission maximum was observed in DHP particles regardless whether $CdCl_2$ or $Cd(NO_3)_2$ was used in the preparation of colloids. Conversely, differences between hexametaphosphate-stabilized CdS particles, prepared from these two precursors in water, were claimed to exist.[52] Those prepared from $CdCl_2$ had emission maximum at 522 nm. This was attributed to hole trapping by the electron adduct of interstitial sulfur, I_s^-

$$H^+ + I_s^- \rightarrow I_s + h\nu \qquad (3)$$

formed in the substitutional doping of CdS by Cl^-.[52] Unlike in water, Cl^- (or other anions) could not penetrate into the vesicle-stabilized colloidal CdS. Electrostatic repulsions between Cl^- and the negatively charged DHP surface precluded this substitution.

Electron acceptors, A (MV^{2+} and Rh^{3+}, for example), efficiently quenched the CdS fluorescence by

$$A + e^- \rightarrow A^- \qquad (4)$$

at the semiconductor surface. Lack of quenching of CdS fluorescence by externally added A (Figures 4 and 6) provided strong evidence against the release of CdS from and the penetration of A into the DHP vesicle interiors. The extent of

(53) Fendler, J. H. *Acc. Chem. Res.* **1976**, *9*, 153–161.
(54) Luisi, P. P. "Biological and Technical Relevance of Reversed Micelles"; Plenum Press: New York, 1983.
(55) Eicke, H. F. *Top. Curr. Chem.* **1980**, *87*, 85–145.
(56) Holsted, R. E.; Aven, M.; Coghill, H. D. *J. Electrochem. Soc.* **1965**, *112*, 177–181.
(57) Heinglein, A. *Ber. Bunsenges. Phys. Chem.* **1982**, *86*, 301–305.
(58) Henglein, A. *J. Phys. Chem.* **1982**, *86*, 2291–2293.
(59) Rosetti, R.; Brus, L. *J. Phys. Chem.* **1982**, *86*, 4470–4472.
(60) Gutierrez, M.; Henglein, A. *Ber. Bunsenges. Phys. Chem.* **1983**, *87*, 474–478.
(61) Kuczynski, J. P.; Milosavljevic, B. H.; Thomas, J. K. *J. Phys. Chem.* **1983**, *87*, 3368–3370.
(62) Henglein, A.; Gutierrez, M. *Ber. Bunsenges. Phys. Chem.* **1983**, *87*, 852–858.
(63) Kuczynski, J.; Thomas, J. K. *J. Phys. Chem.* **1983**, *87*, 5498–5503.

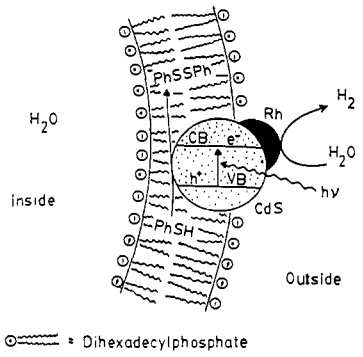

Figure 11. An idealized model for CdS-sensitized water photoreduction by PhSH in aqueous DHP vesicles. The position of the colloid in the vesicle (represented here as generated on the outside surface) is based on fluorescence quenching experiments (Figures 4, 6, and 7).

fluorescence quenching of CdS by cosonicated MV^{2+} was markedly decreased upon 8 days of incubation after CdS formation (Figure 4). This could be interpreted to imply the gradual relocation of the semiconductor into a more hydrophobic environment of the vesicles where there were fewer MV^{2+}. Indeed, gradual penetration of a hydrophobic molecule into surfactant vesicle interiors have been demonstrated recently.[65] Alternatively, aging may have altered one or more of the several equilibria leading to light emission.

Electron donors, D (PhSH, for example), quenched CdS fluorescence by hole transfer from the valence band:

$$D + h^+ \rightarrow D^+ \quad (5)$$

Quenching of DHP-vesicle-entrapped CdS fluorescence by externally added PhSH (Figure 7) indicated the penetration of this hydrophobic electron donor inside of the vesicle bilayers.

The most significant result of the present work was, of course, the successful demonstration of photosensitized water reduction. Following band gap excitation (eq 1), electron–hole recombination (equation 2) could be intercepted at the semiconductor/aqueous vesicle interface. Since the lifetime of the electron–hole pair was extremely short (<1 ns) charge transfer (eq 4 and 5) could only occur at the semiconductor surface. The obvious requirements for efficient charge transfer are large surface area and extensive coverage by electron donors and/or acceptors. These requirements necessitate the presence of small (ca. 40-Å diameter) particles and high concentrations of electron- and/or hole-transfer agents. In homogeneous solutions containing sufficient amounts of oxidants and/or reductants, maintaining such small particles even in the presence of stabilizers (which bound to decrease surface areas and alter redox potentials) is an impossible task. Surfactant vesicles can readily maintain the needed 40-Å diameter colloidal particles (Figure 3) and produce very high local concentrations of reactants.

Conduction band electrons in the CdS particles are thermodynamically capable of water reduction (E_{CB} = +0.36 V vs. NHE):

$$2e^- + 2H^+ \rightarrow H_2 \quad (6)$$

Since this process is kinetically slow it requires a catalyst (Figure 1). Rhodium was used in the present case for promoting reaction 6 at the DHP-vesicle-entrapped CdS–H_2O interface. Rh^{3+}, cosonicated with DHP and Cd^{2+}, is readily reduced,[48] even by visible light in the presence of PhSH. Lack of sufficient data precludes any speculation as to the morphology of the catalytic rhodium particles and their location on CdS. Suffice to say that rhodium is in its reduced form and that there is no hydrogen formation in its absence (Figure 9).

Figure 11 illustrates the mechanism of photosensitized H_2 formation from PhSH in rhodium-coated colloidal CdS in anionic DHP vesicles. The proposed position of the CdS particle (partially buried in the vesicle bilayer) is supported by the following observations: (a) CdS particles generated from externally adsorbed Cd^{2+} ions did not precipitate, even after months; therefore, they had to remain bound to the vesicle interface. (b) CdS fluorescence was efficiently quenched by PhSH, which was located in the hydrophobic membrane; therefore, the colloidal CdS particles had a direct contact with the inner part of the membrane. (c) The CdS particle retained access to the surface where it originated, since entrapped polar electron acceptors such as MV^{2+}, while unable to penetrate the DHP membrane, could also quench the fluorescence of inside-generated CdS particles. However, this quenching decreased with time, showing a gradual penetration of the CdS toward the middle of the bilayer. (d) CdS particles at the vesicle interiors remained on their original side of the membrane, since externally added quencher such as MV^{2+} and Rh^{3+}, while adsorbed on the outside surface of DHP vesicles, did not quench "inside" CdS fluorescence, even after several weeks.

Although quantitative comparisons are difficult to make, initial rates of photosensitized hydrogen production in the present system were comparable to that observed in homogeneous solutions[16] at very much higher CdS and electron-donor (EDTA) concentrations, and they were superior to that reported in reversed micelles.[47]

Accumulation of the oxidized electron donor PhSSPh in the vesicle bilayer was a distinct disadvantage of the present system. Other electron donors are being explored in this and related surfactant-vesicle-stabilized, catalyst-coated, colloidal semiconductors.

Acknowledgment. Support of this work by the Department of Energy is gratefully acknowledged. We are grateful to Arnold J. Drube, Science Research Laboratory, Central Research, 3M Company, St. Paul, MN, for taking the electron micrographs.

(64) Metcalfe, K.; Hester, R. *J. Chem. Soc., Chem. Commun.* **1983**, 133–135.
(65) Nome, F.; Reed, W.; Politi, M.; Tundo, P.; Fendler, J. H. *J. Am. Chem. Soc.*, in press.

Registry No. Rh, 7440-16-6; CdS, 1306-23-6; H_2, 1333-74-0; PhSH, 108-98-5; Rh^{3+}, 16065-89-7; Cd^{2+}, 22537-48-0; H_2S, 7783-06-4; DHP, 2197-63-9; $MVCl_2$, 1910-42-5.